Applied Catalysis B: Environmental 115–116 (2012) 107–116

Contents lists available at SciVerse ScienceDirect

Applied Catalysis B: Environmental

journal homepage: www.elsevier.com/locate/apcatb

Finding the best Fe^{2+}/Cu^{2+} combination for the solar photoelectro-Fenton treatment of simulated wastewater containing the industrial textile dye Disperse Blue 3

Ricardo Salazar[a], Enric Brillas[b], Ignasi Sirés[b,*]

[a] Departamento de Ciencias del Ambiente, Facultad de Química y Biología, Universidad de Santiago de Chile, USACh, Casilla 40, Correo 33, Santiago, Chile
[b] Laboratori d'Electroquímica dels Materials i del Medi Ambient, Departament de Química Física, Facultat de Química, Universitat de Barcelona, Martí i Franquès 1-11, 08028 Barcelona, Spain

ARTICLE INFO

Article history:
Received 8 November 2011
Received in revised form
12 December 2011
Accepted 15 December 2011
Available online 24 December 2011

Keywords:
Anthraquinonic dyes
Boron-doped diamond anode
Metal catalysts
Solar photoelectro-Fenton
Wastewater treatment

ABSTRACT

The performance of the solar photoelectro-Fenton (SPEF) process with Fe^{2+} and Cu^{2+} as metal co-catalysts and its application to the treatment of solutions simulating Disperse Blue 3 (DB3) dye bath effluents of a Chilean textile company are reported in this paper. The trials were carried out with 2.5 l solutions using a solar pre-pilot plant containing an electrochemical reactor with a 20 cm^2 BDD anode and air-diffusion cathode, coupled to a 600 ml solar photoreactor. DB3 solutions with 0.1 M Na_2SO_4 at pH 3.0 were electrolyzed to assess the effect of the applied current density, catalyst nature and concentration and dye content on the decolorization rate, dye removal and total organic carbon (TOC) abatement. The SPEF treatments using 0.5 mM Fe^{2+} + 0.1 mM Cu^{2+} led to the quickest degradation kinetics, mainly due to the concomitant action of UV photolysis and the generated oxidizing hydroxyl radicals on the organic molecules and/or their Cu(II) and Fe(III) complexes. Based on the identification of up to 15 aromatic by-products by GC–MS, a reaction scheme for DB3 degradation has been proposed. The progressive color and TOC removal of DB3 solutions were due to various changes undergone by the initial anthraquinonic structure, including the modification/addition of auxochromes giving 6 anthraquinonic by-products and its cleavage to yield compounds with 2 aromatic rings due to intermolecular cyclization or 1 aromatic ring mainly in the form of phthalic acid derivatives. Upon cleavage of these aromatics, maleic, oxalic, oxamic, pyruvic and acetic acids were formed. NO_3^- ions were released to a larger extent than NH_4^+ ions. The great efficacy of SPEF with Fe^{2+} and Cu^{2+} was demonstrated for simulated wastewater containing DB3 and industrial surfactants and additives at 50 mA cm^{-2}, allowing their total decolorization and almost overall mineralization in only 150 and 360 min, with an energy consumption of 11.0 and 26.4 kWh m^{-3}, respectively.

1. Introduction

The contamination of water bodies by man-made organic chemicals is definitely a critical issue that the recent water framework directives are trying to address in order to ensure good water quality status and healthy ecosystems [1]. Although major attention is paid to persistent and emerging pollutants, especially if they are likely to show endocrine disrupting activity, water pollution by synthetic dyes is also of great concern due to the large worldwide production of dyestuffs. Dyes are extensively used by many industries, mainly in the textile dyeing process, which produces highly contaminating spent dyeing baths containing unreacted dyes, surfactants and additives washed out from the fabric [2]. As a result, the water resources become seriously threatened from the aesthetic and toxicological standpoint, with proven toxic and mutagenic effects [3], which justifies the need for more effective water treatment technologies. Researchers have mainly focused on the removal of azo dyes from water, since they account for about 70% of the world dye production [4]. However, the introduction of synthetic fibres has led to the appearance of some niche markets that require the use of other classes of dyes. For example, disperse anthraquinone dyes such as Disperse Blue 3 (DB3) are neutral species that keep their pre-eminent position for dyeing polyester fibres [5], but their removal from waters has been much less explored.

Since textile wastewaters are toxic, mostly non-biodegradable and resistant to destruction by conventional physicochemical methods, better technologies have been developed to deal with them [6]. Particularly, the advanced oxidation processes (AOPs) have shown an extraordinary ability to reduce their impact. The

* Corresponding author. Tel.: +34 934021223; fax: +34 934021231.
E-mail address: i.sires@ub.edu (I. Sirés).

0926-3373/$ – see front matter © 2011 Elsevier B.V. All rights reserved.
doi:10.1016/j.apcatb.2011.12.026

AOPs are environmentally-friendly chemical, photochemical, photocatalytic or electrochemical oxidation methods involving the on-site generation of highly reactive oxygen species (ROS) such as (primarily but not exclusively) hydroxyl radicals (•OH) that control the degradation mechanism [7].

Over the past 20 years, several electrochemical separation and degradation technologies have been devised or enhanced for the remediation of wastewaters [8]. Among them, the electrochemical AOPs (EAOPs) are highly appreciated because they allow the production of large amounts of •OH by simply controlling the applied current, although some disadvantages must be overcome [9]. Electro-oxidation or anodic oxidation (AO) is the most popular technique due to its simplicity. In this method, the pollutants are oxidized by (i) direct electron transfer to the anode and/or (ii) mediated oxidation with heterogeneous ROS formed from water discharge at the anode surface [10]. At present, boron-doped diamond (BDD) is the best anode material to oxidize organic pollutants like synthetic dyes [11–16], since it yields a high concentration of physisorbed hydroxyl radicals (BDD(•OH)) at a very positive anode potential [17] from reaction (1):

$$BDD + H_2O \rightarrow BDD(^{\bullet}OH) + H^+ + e^- \quad (1)$$

The oxidation can be significantly accelerated by using additional catalysts, giving rise to two main groups of processes [18]: (i) photoelectrocatalysis, by combination with heterogeneous photocatalysts, and (ii) Fenton-based methods, by combination with homogeneous catalysts.

In recent years, our group has developed several Fenton-based technologies such as the electro-Fenton (EF) process. The most spread setup includes an electrolytic cell where H_2O_2 is continuously produced in the contaminated acidic solution from the two-electron cathodic reduction of O_2. Carbonaceous cathodes including graphite [19], gas-diffusion electrodes [20–22], carbon or graphite felts [23–28], carbon cloth [29], activated carbon fibre [30] and carbon nanotubes [31,32] have been used in EF because they exhibit a high efficiency for this reaction. In addition, EF requires the presence of low amounts of Fe^{2+} ions as catalyst to electrogenerate •OH in the bulk from Fenton's reaction with $k_2 = 63\ M^{-1}\ s^{-1}$ [18]:

$$Fe^{2+} + H_2O_2 \rightarrow Fe^{3+} + {}^{\bullet}OH + OH^- \quad (2)$$

Therefore, in the EF treatment with a BDD anode, the refractory organic molecules and their metal complexes can be oxidized by the combined action of BDD(•OH) formed at the anode from reaction (1) and •OH produced in the bulk from reaction (2). Some attempts have also been made to show the possible (co-)catalytic action of Cu^{2+}. A positive synergistic effect of all catalysts, which promotes a quicker decontamination, has been observed due to the formation of specific Cu(II)-carboxylate complexes like Cu(II)-oxamate that can be destroyed by •OH [20].

The alternative process called photoelectro-Fenton (PEF) is even more effective than EF [18]. In PEF with a BDD anode, the solution is treated under EF conditions and simultaneously irradiated with UV light to accelerate the degradation rate of organics. The much higher performance of this process is due to several concomitant reactions: (i) the production of BDD(•OH) on the anode and •OH in the bulk, (ii) the photoreduction of Fe(III) (as $[Fe(OH)]^{2+}$) formed in reaction (2), which yields additional •OH and regenerates Fe^{2+}, as shows reaction (3), and (iii) the quick photolysis of Fe(III)-carboxylate by-products that are quite refractory to the oxidation mediated by hydroxyl radicals [18].

$$[Fe(OH)]^{2+} + h\nu \rightarrow Fe^{2+} + {}^{\bullet}OH \quad (3)$$

A clear disadvantage of the PEF system is the excessive economical cost arising from the use of commercial lamps, because the minimization of the economical requirements is mandatory to introduce the newly developed water remediation technologies in large scale systems. Consequently, a much more appealing PEF process is being developed by our group. It is called solar photoelectro-Fenton (SPEF) since it uses sunlight as a free and renewable UV/Vis source, combined with Pt/gas diffusion or BDD/gas diffusion electrochemical reactors. Previous work revealed the excellent results obtained for cresols [33], pharmaceuticals [34–36] and three azo dyes, namely Acid Yellow 36, Disperse Red 1 and Disperse Yellow 3 [37,38]. However, some issues have not been explored yet in SPEF: (i) the (co-)catalytic effect of other metal ions apart from Fe^{2+} and (ii) the behavior of anthraquinonic structures, which may involve some particular reaction pathways.

In this paper, the SPEF treatment of DB3 has been carried out using the aforementioned solar pre-pilot plant with a BDD/air diffusion reactor at constant current density. DB3 is of great industrial interest because it is used by textile dyehouses such as the Chilean one mentioned in this work. As far as we know, there are no studies reporting the degradation of this dye by AOPs, although some authors have reported the treatment of other anthraquinone dyes such as Acid Green 25, Mordant Red 3 and 11, Reactive Blue 4, 19 and 49, Reactive Brilliant Blue X-BR and Remazol Brilliant Blue R by electro-oxidation [12,15,16,39–41], EF [21,42], chemical Fenton [43], O_3 [44] and TiO_2 photocatalysis [42,45–47]. First, acidic DB3 solutions were electrolyzed to assess the effect of current density and Fe^{2+} and dye concentrations on the decolorization rate, DB3 decay and total organic carbon (TOC) abatement. Cu^{2+} was further used to examine the performance of the co-catalyzed SPEF process, which is a very interesting possibility because Chile is the world's largest producer of copper. A careful analysis of the degradation by-products was made by high-performance liquid chromatography (HPLC), ion chromatography (IC) and gas chromatography-mass spectrometry (GC–MS) to provide a detailed discussion on the reaction pathways. Finally, textile wastewaters that simulated the real dye bath effluents were prepared and treated by SPEF under the best catalytic conditions previously found. This is an essential preliminary step towards the applicability of the SPEF process for the treatment of real wastewaters in a future pilot plant.

2. Experimental

2.1. Chemicals

DB3 (1-[(2-hydroxyethyl)amino]-4-(methylamino)-9,10-anthracenedione, $C_{17}H_{16}N_2O_3$, C.I. 61505, dye content 75%) and all the surfactants and additives (Antimussol, Rucolin JES, Verolan, Levacid AS and Parilan HT) needed for the preparation of the synthetic dye formulation wastewater, were supplied by Textile Monarch S.A. (Santiago, Chile) and were used as received. Maleic, oxalic, oxamic and pyruvic acids were of analytical grade from Merck and Avocado. Anhydrous sodium sulfate used as background electrolyte, and iron(II) sulfate heptahydrate and copper(II) sulfate pentahydrate used as (co-)catalysts, were analytical grade from Merck and Fluka. Solutions were prepared with deionized water and their pH was adjusted with analytical grade sulfuric acid from Merck. Organic solvents and other chemicals used were either HPLC or analytical grade from Merck, Fluka and Avocado.

2.2. Solar pre-pilot plant

For each trial, 2.5 l of solution were introduced into the reservoir and recirculated through the system by means of a magnetic drive centrifugal pump from Iwaki at a liquid flow rate of 200 l h^{-1} regulated by a flowmeter. The solution further passed through two heat exchangers to maintain the temperature at 35 °C, the electrochemical reactor and the solar photoreactor to finally return

to the reservoir. A scheme of the experimental set-up is shown elsewhere [33]. The electrochemical reactor was an undivided filter-press cell containing components of 8 cm × 12 cm in dimension, separated with Viton gaskets to avoid leakage and packed between two larger stainless steel screwed end plates. The anode was a BDD thin film from Adamant Technologies and the cathode was a carbon-polytetrafluoroethylene (PTFE) air-diffusion electrode from E-TEK. A PVC liquid compartment with a central window of 4 cm × 5 cm (20 cm^2) allowed contacting the effluent with the outer faces of both electrodes, with 1.2 cm of interelectrode gap. The inner face of the cathode contacted a Ni mesh employed as electrical connector and was in contact with a PVC gas chamber fed with compressed air at an overpressure of 8.6 kPa regulated with a back-pressure gauge to continuously produce H_2O_2 from cathodic O_2 reduction. The solar photoreactor was a polycarbonate box of 24 cm × 24 cm × 2.5 cm (irradiated volume of 600 ml), connected to the liquid outlet of the cell. It was built-up with a 30°-tilted mirror at the bottom to better collect the sun rays. The solar experiments were performed in sunny and clear days during the summer of 2011 in our laboratory in Barcelona, Spain (latitude: 41° 21′N, longitude: 2° 10′E), with an average UV incident radiation of 30 W m^{-2}, measured with a Kipp & Zonen CUV 5 radiometer. The comparative EF trials were performed in the dark by covering the plant with an opaque cloth. Previous work showed the great ability of the BDD/air diffusion cell for H_2O_2 generation, since 18 mM of this compound were accumulated in 2.5 l of a 0.1 M Na_2SO_4 solution of pH 3.0 after 240 min of electrolysis at 50 mA cm^{-2} and 35 °C [37].

Freshly prepared solutions of 200 mg l^{-1} DB3 (100 mg l^{-1} TOC) in 0.1 M Na_2SO_4 at pH 3.0, with or without Fe^{2+} and Cu^{2+} as (co-)catalysts, were comparatively degraded by solar anodic oxidation with electrogenerated H_2O_2 (AO-H_2O_2), EF and SPEF in the pre-pilot plant. The pH 3.0 was selected because it has been found the optimal for the analogous treatments of other aromatics [18]. The effect of the applied current density was tested at 15, 30, 50 and 80 mA cm^{-2}, resulting in average cell voltages of 7.7, 9.2, 11.0 and 14.3 V, respectively, whereas the influence of the dye concentration was examined for 100–400 mg l^{-1} DB3 (50–200 mg l^{-1} TOC), which are typical contents in industrial wastewaters. For the SPEF treatments of simulated wastewaters, solutions were prepared according to the composition of industrial dye bath effluents from Textile Monarch S.A.: 0.5 ml of the antifoaming agent Antimussol, 2.5 ml of the running crease inhibitor Rucolin JES, 2.5 ml of the complexing agent Verolan, 0.4 ml of the buffer Levacid AS and 2.5 ml of the color guard Parilan HT. All these solutions contained 0.1 M Na_2SO_4 to provide enough electrical conductivity.

2.3. Apparatus and analysis procedures

Constant current electrolyses were performed with an Agilent 6552A DC power supply, which also displayed the cell voltage. The solution pH was measured with a Crison 2000 pH-meter. Samples were always withdrawn at regular time intervals from the solution kept in the reservoir, then alkalinized to stop the degradation process and finally microfiltered with 0.45 μm PTFE filters from Whatman before analysis. The decolorization of DB3 solutions was monitored from the absorbance (A) decrease at the maximum visible wavelength (λ_{max}) of 710 nm, measured from the spectra recorded on a Shimadzu 1800 UV/Vis spectrophotometer at 35 °C. The mineralization of these solutions was monitored from the decay of their TOC determined on a Shimadzu VCSN TOC analyzer. Reproducible TOC values with an accuracy of ±1% were always found by injecting 50 μl aliquots to the analyzer. From these data, the energy consumption per unit TOC mass (EC_{TOC}) and per unit volume (EC) were then calculated from Eqs. (4) and (5), respectively [18]:

$$EC_{TOC}\,(\text{kWh}\,(\text{kg TOC})^{-1}) = \frac{1000 E_{cell}\, I\, t}{(\Delta \text{TOC})_{exp}\, V_s} \quad (4)$$

$$EC\ (\text{kWh m}^{-3}) = \frac{E_{cell}\, I\, t}{V_s} \quad (5)$$

where E_{cell} is the average cell voltage (V), I is the applied current (A), t is the electrolysis time (h), $(\Delta \text{TOC})_{exp}$ is the experimental TOC decay (mg l^{-1}) and V_s is the volume of the treated solution (l).

The decay of DB3 with electrolysis time was followed by reversed-phase HPLC using a Waters 600 LC fitted with a Spherisorb ODS2 5 μm, 15 cm × 4.6 mm (i.d.), column at room temperature, and coupled with a Waters 996 photodiode array detector selected at λ = 710 nm. The analyses were carried out isocratically by using a 50:50 (v/v) acetonitrile/water (1.0 mM ammonium acetate, pH 3.0) mixture at 1.0 ml min^{-1} as mobile phase. The generated aliphatic carboxylic acids were identified and quantified by ion-exclusion HPLC with the same LC, but fitted with a Bio-Rad Aminex HPX 87H, 30 cm × 7.8 mm (i.d.), column at 35 °C, and setting the detector at λ = 210 nm. The mobile phase was 4 mM H_2SO_4 at 0.6 ml min^{-1}. Absorption peaks with retention times (t_R) of 14.0 min for DB3 and 6.9, 8.2, 9.1 and 9.6 min for oxalic, maleic, pyruvic and oxamic acids were obtained in the corresponding chromatograms. Released inorganic ions were quantified by IC using a Shimadzu LC 10Avp instrument coupled with a Shimadzu CDD 10Avp conductivity detector. The NO_3^- concentration in electrolyzed solutions was obtained with a Shim-Pack IC-A1S, 10 cm × 4.6 mm (i.d.), anion-exchange column at 40 °C and a mobile phase consisting of 1.0 mM *p*-hydroxybenzoic acid and 1.1 mM *N*,*N*-diethylethanolamine circulating at 1.5 ml min^{-1}. The NH_4^+ concentration was determined with a Shodex IC YK-421, 12.5 mm × 4.6 mm (i.d.), cation-exchange column at 40 °C and a mobile phase with 5.0 mM tartaric acid, 2.0 mM dipicolinic acid, 24.2 mM boric acid and 15.0 mM crown ether circulating at 1.0 ml min^{-1}.

The aromatic by-products were identified by GC–MS using an Agilent Technologies system composed of a 6890N gas chromatograph equipped with a 7683B series injector and a 5975 mass spectrometer in EI mode at 70 eV. Nonpolar Agilent J&W DB-5 and polar HP INNOWax columns, both with dimensions of 0.25 μm, 30 m × 0.25 mm (i.d.), were used. The temperature ramp was: 36 °C for 1 min, 5 °C min^{-1} up to 300 °C and hold time 10 min. The temperature of the inlet, source and transfer line was 250, 230 and 280 °C, respectively. The analyses were made by splitless (0.7 min) injection. Aiming to identify as many reaction intermediates as possible, solutions of 200 mg l^{-1} DB3 were electrolyzed under different conditions during short and long time periods. Several analytical procedures were then applied to the final solutions in order to get a complete set of samples: (i) solvent extraction employing 100 ml of CH_2Cl_2 in five times, followed by drying of the organic fraction with anhydrous Na_2SO_4, filtration and final concentration under reduced pressure, (ii) the same procedure but including a derivatization step using a small volume of acetic anhydride prior to final concentration and (iii) the same treatment but using ethyl acetate to obtain the corresponding ethylated derivatives.

3. Results and discussion

3.1. Effect of the experimental parameters on the mineralization of synthetic DB3 solutions

The effect of the operating conditions on the performance of the SPEF treatment of DB3 was firstly assessed by studying the mineralization trends. The electrolyses were always carried out with 2.5 l of aqueous solutions of DB3 in 0.1 M Na_2SO_4, at pH 3.0, 35 °C and

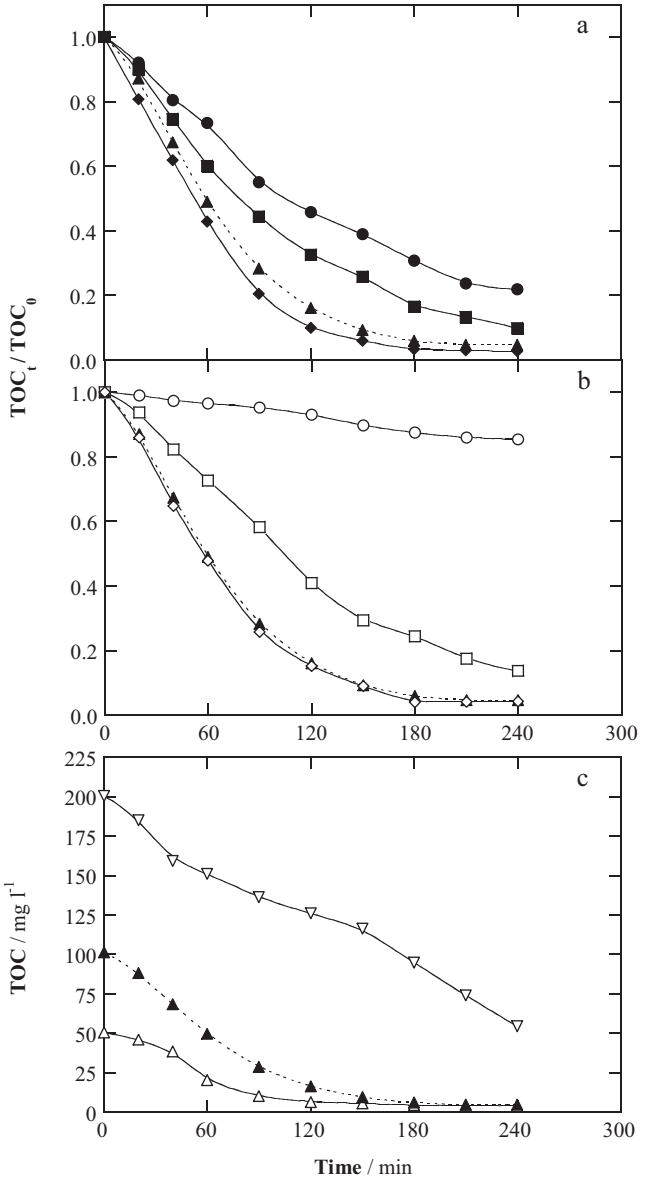

Fig. 1. Effect of experimental variables on the SPEF degradation with electrolysis time for 2.5 l of solutions of the dye DB3 in 0.1 M Na_2SO_4 at pH 3.0 and 35 °C using a flow plant with a BDD/air diffusion cell coupled with a solar photoreactor at 200 l h^{-1}. (a) Normalized TOC decay for 200 mg l^{-1} DB3 with 0.5 mM Fe^{2+} at: (●) 15 mA cm^{-2}, (■) 30 mA cm^{-2}, (▲) 50 mA cm^{-2} and (♦) 80 mA cm^{-2}. (b) Normalized TOC decay for 200 mg l^{-1} DB3 (○) without catalyst (solar AO-H_2O_2 process) and with (□) 0.25 mM, (▲) 0.5 mM and (◊) 1.0 mM Fe^{2+} at 50 mA cm^{-2}. (c) TOC removal for (△) 100 mg l^{-1}, (▲) 200 mg l^{-1} and (▽) 400 mg l^{-1} DB3 with 0.5 mM Fe^{2+} at 50 mA cm^{-2}.

200 l h^{-1}, yielding the results shown in Fig. 1a–c. For all these trials, the solution pH remained almost unchanged, attaining a final value of ca. 2.8. This is an important finding in view of the future scale-up of this technology because self-adjustment of pH simplifies the treatment and makes it more cost-effective.

Fig. 1a depicts the effect of the applied current density in the range of 15–80 mA cm^{-2} for solutions containing 200 mg l^{-1} DB3 and 0.5 mM Fe^{2+}. In all cases, TOC decreased progressively with prolonged electrolysis time. After 240 min, 22% TOC was still remaining in solution at the lowest current density of 15 mA cm^{-2}, although the profile of this curve suggests that a higher TOC abatement might be achieved within some hours. When working at 30 mA cm^{-2}, only 10% TOC was present in solution after the same period, whereas almost overall mineralization (>95% TOC removal) was attained at 50 mA cm^{-2}. A faster mineralization can then be observed as the current rises. However, a higher value of 80 mA cm^{-2} only led to the acceleration during the first stages, with 50% TOC removal in less than 60 min, being the final stage very similar to that of 50 mA cm^{-2}. The high efficacy of the SPEF process with Fe^{2+} for the degradation of DB3 and its reaction by-products can be mainly ascribed to the combined action of sunlight irradiation and the BDD(•OH) and •OH formed at the anode and in the bulk, respectively, over the organic molecules and their Fe(II) and/or Fe(III) complexes. Therefore, the mineralization enhancement as current increases can be explained by the larger direct (controlled by the anodic electron transfer) and indirect (controlled by the cathodic O_2 reduction) production of hydroxyl radicals. Other electrogenerated species such as $S_2O_8^{2-}$ ions and ROS like O_3, H_2O_2 and hydroperoxyl radical (HO_2•) [18] play a negligible role in this EAOP owing to their much lower oxidation power and/or poorer concentration in the bulk. In contrast, their contribution, as well as that of direct electro-oxidation at the BDD surface and cathodic electoreduction, have been proven an important route in the non-Fenton electrochemical remediation of anthraquinones [4,15]. From these results, 50 mA cm^{-2} was selected as the most suitable current density value for further experiments. Higher values led to an excessive current waste with a higher cost, since the mass transport limitations prevent the organic matter to encounter the excess of BDD(•OH) and •OH produced, which can then easily self-react with plenty of surrounding hydroxyl radicals or can be wasted in other parasitic reactions involving other reactive species like H_2O_2, Fe^{2+}, etc. [18].

Fig. 1b presents the effect of the Fe^{2+} concentration in the range of 0–1.0 mM. In the absence of Fe^{2+} (solar AO-H_2O_2 process), the normalized TOC decay was very poor, with 85% TOC still remaining after 240 min. Under these conditions, the organic molecules are primordially oxidized by BDD(•OH) and thus, the mineralization reactions are given to a small extent because they are limited to a confined region of the whole volume. In contrast, the addition of a catalytic amount of Fe^{2+} allowed to work under SPEF conditions, which led to a high rate and degree of mineralization. For example, only 14% TOC remained in the final solution upon use of 0.25 mM Fe^{2+}, as a result of the large amounts of the more active •OH produced by reactions (2) and (3) and the action of natural UV radiation on the by-products and their iron complexes. A much quicker TOC removal was achieved by using 0.5 mM Fe^{2+}, with almost total mineralization at 240 min. This can be mainly explained by the enhancement of three kinds of reactions involving the iron species: (i) the formation of more •OH in the bulk, because the largely electrogenerated H_2O_2 can react more rapidly with such an amount of Fe^{2+} according to Fenton's reaction (2) [37], (ii) the additional •OH formation induced by $[Fe(OH)]^{2+}$ photoreduction according to reaction (3) and (iii) the photodecarboxylation of Fe(III)-carboxylate complexes. Finally, the use of 1.0 mM Fe^{2+} did not improve the results found for 0.5 mM Fe^{2+}, because the beneficial contribution to the three previous reactions is negatively compensated by the significant destruction of •OH upon reaction with Fe^{2+} [18]. As a result, 0.5 mM Fe^{2+} was used for subsequent experiments.

The influence of the initial DB3 concentration on TOC removal can be seen in Fig. 1c. All the solutions could be degraded at a high rate reaching almost overall mineralization at long electrolysis time. At 240 min, for example, 46, 96 and 146 mg l^{-1} TOC were already removed from starting solutions containing 50, 100 and 200 mg l^{-1} TOC (100, 200 and 400 mg l^{-1} DB3), respectively. Thus, TOC was reduced by 93%, 95% and 73%, proving a gradual loss in percentage of TOC removal when rising the dye content, especially from 100 to 200 mg l^{-1} TOC. This can be simply explained by the presence of a much larger quantity of initial and generated organic molecules, then requiring a longer time to disappear. Nevertheless, an increase in dye concentration accelerates the TOC removal rate

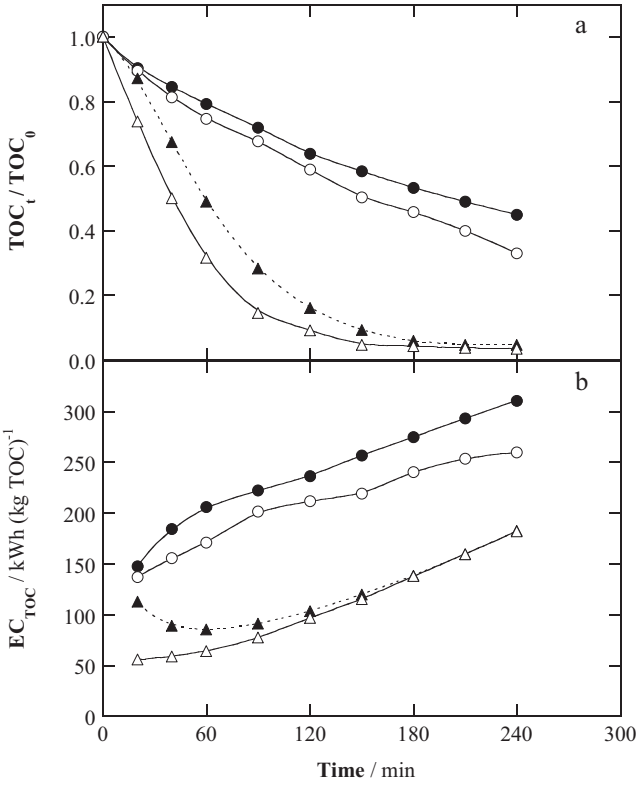

Fig. 2. (a) Normalized TOC abatement and (b) energy consumption per unit TOC mass vs electrolysis time for the treatment of 2.5 l of 200 mg l^{-1} DB3 solutions with 0.1 M Na_2SO_4 containing (●, ▲) 0.5 mM Fe^{2+} or (○, △) 0.5 mM Fe^{2+} + 0.1 mM Cu^{2+} at pH 3.0, 50 mA cm^{-2}, 35 °C and 200 l h^{-1}. Process: (●, ○) EF and (▲, △) SPEF.

(the amount of organic matter that is removed per time period), owing to the decrease in rate of the parasitic reactions that waste •OH in worthless events.

The above findings demonstrate the high degradation ability of the SPEF with Fe^{2+} for the treatment of an anthraquinonic dye, confirming previous results obtained for azo dyes [37,38]. Note that among previous studies dealing with the electrochemical mineralization of anthraquinone dyes solutions, only EF [21] and electro-oxidation with high oxidation power anodes such as BDD and doped PbO_2 [12,15] had led to an abatement of more than 90% of their organic matter content.

3.2. Performance of the SPEF treatment catalyzed by Fe^{2+} and Cu^{2+}

Aiming to improve the positive results shown above for the SPEF degradation with Fe^{2+}, the (co-)catalytic effect of Cu^{2+} was explored. Fig. 2a reveals the influence of two key parameters in this EAOP. First, the effect of sunlight irradiation is shown by comparing the EF treatment of solutions containing 200 mg l^{-1} DB3 and 0.5 mM Fe^{2+} at 50 mA cm^{-2} with the analogous SPEF process. EF led to a much slower TOC removal, with 45% TOC still remaining in solution at 240 min. This confirms the fundamental role of sunlight irradiation in the aforementioned photoreduction and photodecarboxylation reactions, because in dark (EF) conditions the •OH can only very slowly degrade some refractory by-products and iron complexes. The (co)-catalytic effect of Cu^{2+} is also surveyed in Fig. 2a. The nature of the catalyst can definitely become the most crucial parameter determining the electrolysis performance in Fenton's reaction chemistry. Our group clearly showed this for the EF and PEF treatment of paracetamol [20], nitrobenzene [48] and Indigo Carmine [49], but not yet for SPEF. The positive synergistic effect of Fe^{2+} and Cu^{2+} that promoted the quickest mineralization was accounted for by the easier oxidation of some nitrogenated complexes of Cu(II) compared with the competitively formed Fe(III) complexes, that are more slowly removed. Moreover, Cu^+ can be formed from the reduction of Cu^{2+} with HO_2• by reaction (6) with $k_2 = 5.0 \times 10^7$ M^{-1} s^{-1} and/or with organic radicals R• by reaction (7) [20,50]:

$$Cu^{2+} + HO_2^{\bullet} \rightarrow Cu^{+} + H^{+} + O_2 \quad (6)$$

$$Cu^{2+} + R^{\bullet} \rightarrow Cu^{+} + R^{+} \quad (7)$$

Then, the Cu^{2+}/Cu^+ couple can contribute to the production of •OH in the bulk from the Fenton-like reaction (8) with $k_2 = 1.0 \times 10^4$ M^{-1} s^{-1} and to the regeneration of Fe^{2+} from reaction (9), which prolongs the Fe^{3+}/Fe^{2+} catalytic cycle involved in Fenton's reaction (2) [50]:

$$Cu^{+} + H_2O_2 \rightarrow Cu^{2+} + {}^{\bullet}OH + OH^{-} \quad (8)$$

$$Cu^{+} + Fe^{3+} \rightarrow Cu^{2+} + Fe^{2+} \quad (9)$$

Several concentrations of Cu^{2+} were tested up to find that 0.1 mM was the optimal one. The synergistic effect of this ion as (co)-catalyst is evident in Fig. 2a, where both the EF and SPEF treatments became accelerated in the presence of both ions (Fe^{2+}/Cu^{2+}). Thus, in EF, only 33% TOC was remaining in solution at 240 min. In SPEF, the almost complete TOC removal at the end of the electrolysis was reached after experiencing a faster mineralization during the first 180 min compared to SPEF with only Fe^{2+}. At 40 min, for example, 50% and 33% TOC removal were attained for SPEF with Fe^{2+}/Cu^{2+} and Fe^{2+}, respectively. Since the effect of Cu^{2+} was found even in the dark, it can be concluded that the sunlight irradiation plays a secondary role in the Cu^{2+}-catalyzed reactions, in contrast to that observed for the Fe^{2+}-catalyzed reactions. This suggests that the quicker mineralization of DB3 solutions in SPEF catalyzed by Fe^{2+}/Cu^{2+} mainly arises from reactions (8) and (9) and/or the easier oxidation of complexes of Cu(II) with nitrogenated intermediates by •OH [20].

The EC_{TOC} calculated for the four processes of Fig. 2a according to Eq. (4) is shown in Fig. 2b. After 240 min, higher consumptions of 311 and 260 kWh (kg TOC)$^{-1}$ were required in EF with Fe^{2+}/Cu^{2+} and Fe^{2+}, respectively, as expected from their much lower mineralization ability than the SPEF treatments, which required 182 kWh (kg TOC)$^{-1}$ (17.6 kWh m^{-3}). Considering the value of the industrial kWh in Spain (0.06–0.17 € [51]), the energy cost for the overall mineralization of DB3 solutions by SPEF was 1.06–2.99 € m^{-3}. Obviously, in real-scale applications, coupling of SPEF with other technologies could reduce the mineralization cost. In all cases, the EC_{TOC} values were lower during the first stages, but the gradual deceleration of the degradation rate observed in Fig. 2a due to mass transport limitations and the generation of more refractory molecules caused the concomitant increase of EC_{TOC}. A slightly lower consumption of 150 kWh (kg TOC)$^{-1}$ (14.2 kWh m^{-3}) was reported for the analogous SPEF treatment with Fe^{2+} of disperse azo dyes Disperse Red 1 and Disperse Yellow 3 [38]. It is then clear that the structure of the pollutant and the presence of different functional groups may exert influence on the performance and efficiency of the electrochemical process, as also found by Saez et al. [15].

When treating dye solutions, it is important to assess the ability of the process to remove the color, which is their most immediate polluting effect. The color removal for the EF and SPEF processes of Fig. 2a is represented in Fig. 3a as the drop of the A_t/A_0 ratio (normalized absorbance) at 710 nm along the electrolysis time. The UV/Vis spectrum of DB3 is included in the inset panel, where two main absorption bands can be observed. The band centred at 254 nm is related to the anthraquinonic structure (quinoid absorption), typical for the $\Pi \rightarrow \Pi^*$ aromatic transitions of the aromatic moieties,

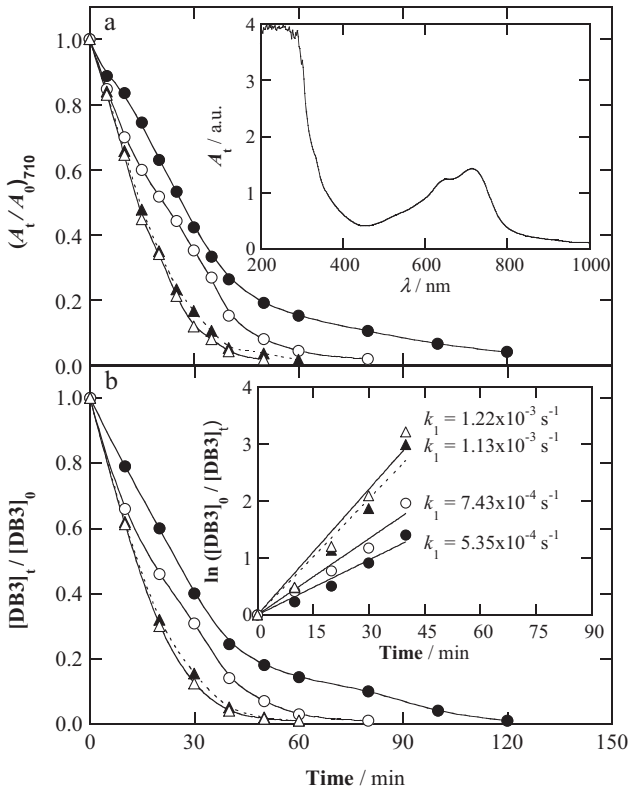

Fig. 3. Time course of the (a) normalized absorbance at 710 nm and (b) normalized DB3 concentration for the EF and SPEF trials of Fig. 2. The inset panel in plot (a) shows the absorption spectrum for the initial 200 mg l^{-1} DB3 solution. The inset panel in plot (b) presents the kinetic analysis assuming a pseudo first-order reaction for the dye and the corresponding rate constants obtained.

whereas the band with a maximum absorption at 710 nm is due to the side chains that are responsible for the blue color. A smaller band with maximum at 625 nm could also be observed, but the greater intensity of the characteristic band at 710 nm was more suitable to carry out the decolorization studies within the visible range. The intensity of all the absorption bands decreased continuously and very rapidly by EF and SPEF, which suggests that different reaction pathways may coexist, involving the simultaneous alteration of the anthraquinonic structure and the auxochromes.

Fig. 3a shows that the normalized absorbance progressively decreased as all electrolyses were prolonged, so that the percentage of color removal increased up to reaching ≥99% at 120, 80, 60 and 50 min in EF with Fe^{2+}, EF with Fe^{2+}/Cu^{2+}, SPEF with Fe^{2+} and SPEF with Fe^{2+}/Cu^{2+}, respectively. The initial dark blue solutions consecutively turned into greenish/bluish, pale green, and pale yellow prior to become colorless. Blank experiments did not show a significant decolorization of the sunlight-irradiated DB3 solution (not shown), thus confirming the expected high stability of anthraquinone dyes to light-induced fading due to their fused aromatic structure. In contrast to the findings for mineralization shown in Fig. 2a, Cu^{2+} has a very positive effect only in the decolorization by EF. This means that in the decolorization stage, the importance of Cu^{2+} is related to the production of a higher concentration of •OH due to the additional action of reactions (8) and (9). The influence of Cu^{2+} is then scarce in SPEF because the sunlight-induced photoreduction of $[Fe(OH)]^{2+}$ by reaction (3) becomes much more relevant.

By analyzing the UV/Vis spectra of electrolyzed solutions, the presence of residual absorbance at 254 nm was observed even when the absorbance at 710 nm became zero. This is related to the presence of persistent aromatic by-products that contribute to the remaining TOC shown in Fig. 2a. Such aromatic intermediates were also found during the treatment of anthraquinone dyes by TiO_2 photocatalysis [45]. The GC–MS study presented in section 3.3 allowed the identification of some of these colorless aromatic compounds.

It is also interesting to compare the electric energy consumption of SPEF with that reported for the decolorization of anthraquinone dyes by other AOPs. Lizama et al. [52] suggested the comparative use of the energy consumption (in kWh m^{-3}) needed to eliminate 90% of the total solution color. As can be seen in Fig. 3a, a progressively shorter time of 80, 50, 35 and 30 min was required to remove 90% of color by the four processes under study. Then, 2.2 kWh m^{-3} (0.13–0.37 €) were needed for the most potent SPEF process with Fe^{2+}/Cu^{2+} to decolorize 200 mg l^{-1} of DB3, which is very competitive if compared with other treatments. For example, 1.66 kWh m^{-3} were required for decolorizing 25 mg l^{-1} Reactive Blue 19 by electro-oxidation with a Fe,F-doped PbO_2 anode [12], whereas 7.6–22.4 kWh m^{-3} were needed for the TiO_2 photocatalytic treatment of 50 mg l^{-1} of the same dye [52].

The DB3 concentration decay during the same four experiments was monitored by reversed-phase HPLC and the time course of the normalized concentration thus obtained is presented in Fig. 3b. Comparison with Fig. 3a allows concluding that the trends of both, DB3 and total color, up to reaching a removal of ≥99% are almost identical. This is related to the existence of a very insignificant accumulation of colored by-products in solution. The effect of Cu^{2+} on the DB3 destruction is therefore analogous to that commented in Fig. 3a. The kinetic analysis shown in the inset of Fig. 3b demonstrated that all the concentration decays agreed with a pseudo first-order reaction between the DB3 molecules and the oxidizing species, with an excellent fitting in all cases. This confirms that oxidation by •OH is the pre-eminent degradation route in this SPEF system, with a constant concentration being available along the time to react with DB3. This differs from non-Fenton systems such as electro-oxidation, where the role of O_3 or $S_2O_8^{2-}$ ions can be relevant during the destruction of the initial anthraquinone [12].

3.3. Identification of DB3 by-products and proposed reaction pathways

There exists little information on the intermediates formed upon electrochemical treatment of anthraquinone dyes, which makes it difficult to elucidate the routes that are responsible for the color fading and mineralization. Table 1 summarizes up to fifteen aromatic by-products identified by GC–MS after treating solutions of 200 mg l^{-1} DB3 by SPEF catalyzed by 0.5 mM Fe^{2+} + 0.1 mM Cu^{2+} at current density of 50 mA cm^{-2} for different time periods. Three kinds of aromatic by-products can be observed: (i) anthraquinonic compounds with three aromatic rings, (ii) heterocyclic compounds with two aromatic rings, and (iii) phthalic acid derivatives and other compounds with only one aromatic ring.

Based on these findings, a general reaction scheme including different pathways for the formation of all the aromatic by-products is proposed in Fig. 4. Since the generation of these intermediates is simultaneous to the color removal, the kinds of changes that lead to the decolorization of the DB3 solutions can be grouped as follows: (i) pathway A: modification/addition of auxochrome groups, which leads to several anthraquinonic intermediates. The type and positions of the substituents in the molecule determine the hue [5]; and (ii) cleavage of the initial (pathways B, C and D) or modified (B′, C′ and D′) anthraquinone structures to yield intermediates with a lower aromaticity degree.

Pathway A gives rise to six anthraquinones. The addition of the auxochrome group —OH leads to monohydroxylated DB3 with *m/z* 312 (A_1). A similar hydroxylation of the parent anthraquinone was also found during the treatment of Acid Blue 80 by TiO_2

Table 1
Aromatic by-products of DB3 by SPEF treatment identified by GC–MS analysis.

Aromatic rings	Compound	Molecular mass ($g\,mol^{-1}$)	*m/z* fragments	Molecular formula	t_R (min)	Column polarity
3	Monohydroxylated DB3	312	312 (M^+)[a]	$C_{17}H_{16}N_2O_4$	43.2	Nonpolar
	1-[(2-Hydroxyethyl)amino]-9,10-anthracenedione	267	267 (M^+), 249, 227, 207, 171, 159	$C_{16}H_{13}NO_3$	51.0	Nonpolar
	4-(Methylamino)-1-nitroso-9,10-anthracenedione	266	266 (M^+), 249, 234, 220, 85, 57	$C_{15}H_{10}N_2O_3$	51.5	Nonpolar
	1-Hydroxy-4-(methylamino)-9,10-anthracenedione	253	253 (M^+), 236, 226, 208	$C_{15}H_{11}NO_3$	49.0	Nonpolar
	1-(Methylamino)-4-amino-9,10-anthracenedione	252	252 (M^+), 235, 224, 207	$C_{15}H_{12}N_2O_2$	50.4	Nonpolar
	1-Hydroxy-4-amino-9,10-anthracenedione	239	239 (M^+), 207, 183, 117, 57	$C_{14}H_9NO_3$	45.7	Nonpolar
2	2,7-Dimethylquinoline	157	157 (M^+), 142, 128, 115	$C_{11}H_{11}N$	29.3	Polar
	2-Methylquinoline	143	143 (M^+), 128, 115, 101	$C_{10}H_9N$	27.0	Polar
	6-Methylquinoline	143	143 (M^+), 115, 89	$C_{10}H_9N$	28.8	Polar
	Isoquinoline	129	129 (M^+), 102, 75, 51	C_9H_7N	26.5	Polar
1	3-Amino-4-hydroxy-6-(vinylamino)phthalic acid or 6-Amino-4-hydroxy-3-(vinylamino)phthalic acid	238	238 (M^+), 207, 181, 149, 57	$C_{10}H_{10}N_2O_5$	49.4	Nonpolar[b]
	3-Hydroxy-6-(vinylamino)phthalic acid	223	223 (M^+), 207, 193, 167, 149, 57	$C_{10}H_9NO_5$	45.9	Nonpolar[b]
	Diethyl phthalate	222	222 (M^+), 177, 149, 76	$C_{12}H_{14}O_4$	34.7	Polar
	3-(Vinylamino)phthalic acid	207	207 (M^+), 193, 167, 149, 57	$C_{10}H_9NO_4$	44.8	Nonpolar[b]
	5-Hydroxy-2-(methylamino)benzaldehyde	151	151 (M^+), 137, 123, 109, 93, 81	$C_8H_9NO_2$	37.8	Polar

[a] Confirmed by derivatization with acetic anhydride, which yielded a product at 47.1 min showing unequivocal *m/z* fragments of 396 (M^+) and 354.
[b] Also identified with the polar column.

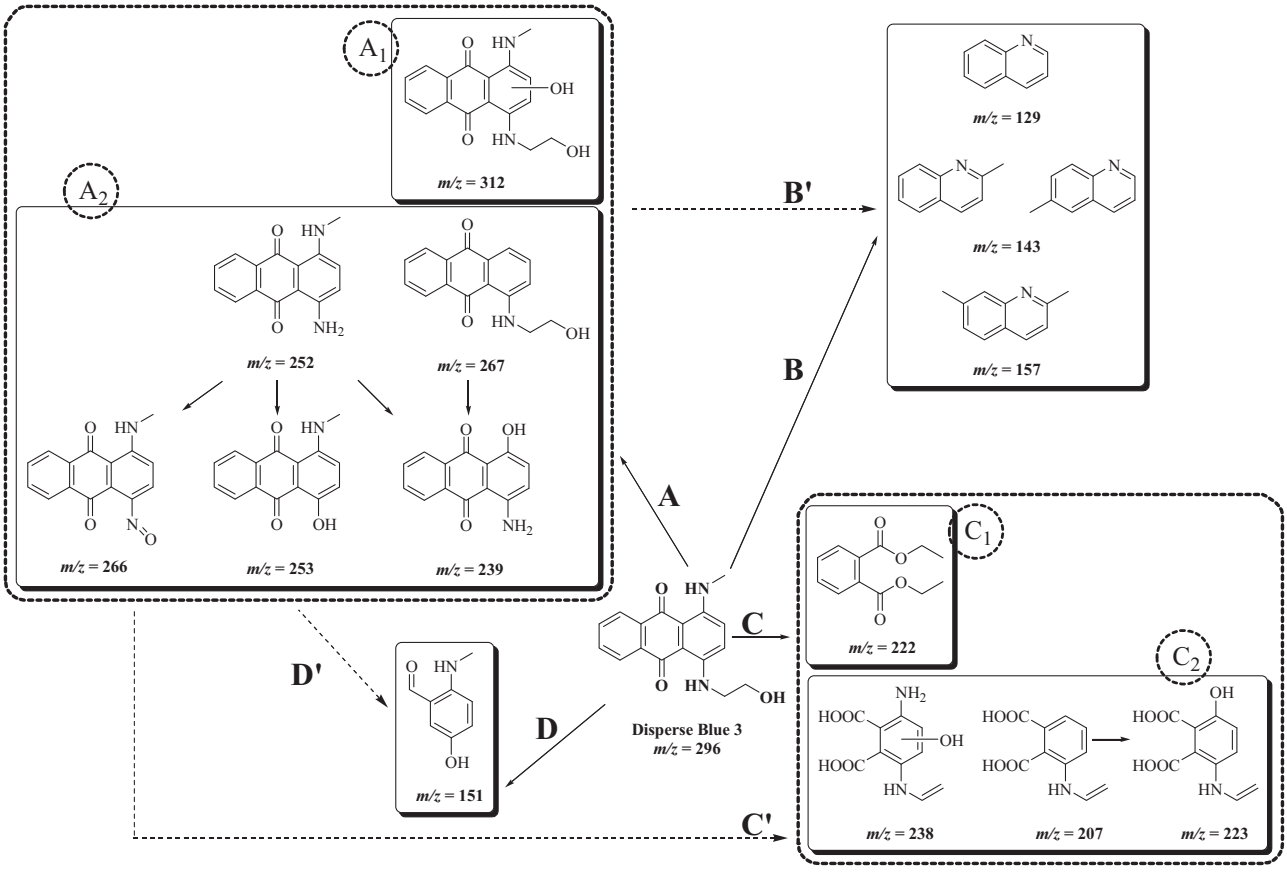

Fig. 4. Proposed reaction pathways for the formation of the aromatic by-products identified by GC–MS during the SPEF treatment of DB3. Number of aromatic rings: (A) 3, (B and B′) 2 and (C, C′, D and D′) 1.

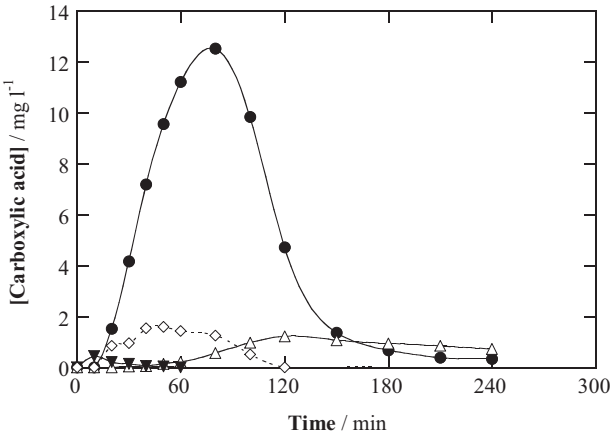

Fig. 5. Evolution of the concentration of the carboxylic acids: (●) oxalic, (△) oxamic, (▼) maleic and (◊) pyruvic detected by ion-exclusion HPLC during the SPEF treatment of 200 mg l^{-1} DB3 with 0.5 mM Fe^{2+} + 0.1 mM Cu^{2+} under the conditions described in Fig. 2.

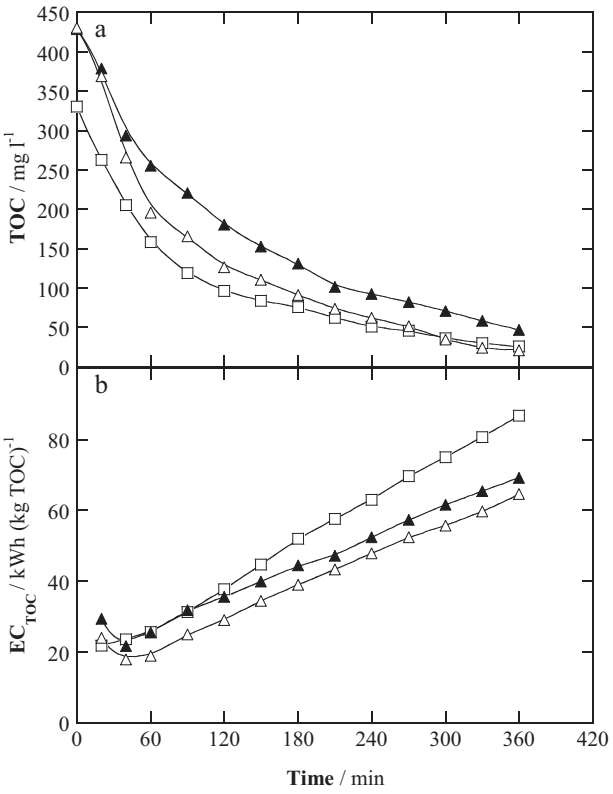

Fig. 6. Variation of (a) TOC and (b) energy consumption per unit TOC mass with electrolysis time for the SPEF treatment of 2.5 l of a simulated textile dyeing wastewater with 0.1 M Na_2SO_4 of pH 3.0 at 50 mA cm^{-2}, 35 °C and 200 l h^{-1}. The solutions contained: (□) 0.5 mM Fe^{2+} + 0.1 mM Cu^{2+}; (▲) 0.5 mM Fe^{2+} and 200 mg l^{-1} DB3; (△) 0.5 mM Fe^{2+} + 0.1 mM Cu^{2+} and 200 mg l^{-1} DB3.

photocatalysis [45]. Other five compounds were formed by modification of the initial auxochromes (A_2). Thus, anthraquinones *m/z* 252 and 267 are formed by partial or total loss of a side chain, respectively. The former involves the breakage of a —$C_{aliphatic}$—N bond (loss of aminoalkyl moiety), whereas the latter arises from the rupture of a —$C_{aromatic}$—N bond. Both of them are followed by proton abstraction. Similar kinds of cleavage of —C—N bonds were suggested for other anthraquinone dyes [40,44,46]. Hydroxylated compounds with m/z 266, 253 and 239 were formed upon hydrolysis or aromatic substitution. Also Kathaee et al. suggested the hydroxylation in —NH_2 position of aminoanthraquinone previously generated from TiO_2 photocatalysis of Acid Green 25 [47].

Pathway B (and similarly B′) yields four heterocyclic compounds with two aromatic rings due to complex, simultaneous bond ruptures followed by intermolecular cyclization. The MS spectra corresponded to the proposed isoquinoline and quinolines with a probability > 85% according to the NIST database. Other authors also hypothesized the formation of heterocycles during the degradation of Reactive Blue 19, such as phthalimide and isoindoline in electro-oxidation [40,41] and a quinoline in ozonation [41].

Pathways C and D (and similarly C′ and D′) lead to the formation of four phthalic acid derivatives and a non-phthalic acid derivative, respectively. They are formed after cleavage at the bonds bearing the —C=O groups, with formation of hydroxyl functional groups (pathways C and C′) and aldehydes (pathways D and D′ to form a compound with *m/z* 151). In pathways C and C′, the appearance of several phthalate-like by-products was confirmed by the unequivocal fragment with *m/z* 149, which corresponded to a protonated phthalic acid anhydride generated by dehydration of phthalic acid derivatives. Diethyl phthalate, with *m/z* 222 (pathway C_1), preserves the benzenic ring and has been reported for another anthraquinone [42]. On the other hand, three intermediates maintain the aminobenzenic side (pathway C_2). Several phthalic acid derivatives, either maintaining the benzenic or aminobenzenic ring, were reported elsewhere for the advanced oxidation of Reactive Blue 19 and Alizarin Red [21,40,44,47].

The cleavage of all the previous aromatic rings leads to the formation of short-chain aliphatic carboxylic acids, which contribute to the residual TOC shown in Fig. 2a once DB3 has disappeared. The GC–MS analyses using a polar column allowed the detection of acetic acid (t_R = 15.6 min, *m/z* = 60 (M^+), 45, 43). The ion-exclusion HPLC analyses of electrolyzed solutions revealed the presence of more persistent oxalic, maleic, pyruvic and oxamic acids, whose time course for the SPEF treatment with Fe^{2+}/Cu^{2+} is shown in Fig. 5. Oxalic acid was accumulated up to a maximum concentration of 12.5 mg l^{-1} at 80 min, whereas the other acids were accumulated to a smaller extent, attaining maximum values of 0.4, 1.6 and 1.22 mg l^{-1} for maleic, pyruvic and oxamic acids at 10, 50 and 120 min, respectively. Oxalic and oxamic are the ultimate carboxylic acids prior to transformation into CO_2 [20]. All the acids were almost totally degraded after 240 min, thus confirming the almost overall mineralization achieved by SPEF catalyzed by Fe^{2+}/Cu^{2+}. In previous sections, the action of Cu^{2+} was focused on the formation of complexes with nitrogenated by-products that can be more easily oxidized. Results of Fig. 5 exemplify that oxamic acid is one of those by-products, since its Cu(II) complexes can be oxidized by •OH [20]. In contrast, the main effect of sunlight is given over the competitively formed, photosensitive Fe(III)-oxalate complexes [18].

The mineralization process is always accompanied by the release of inorganic ions. The IC analyses of the above electrolyzed solutions showed the formation of nitrogenated inorganic ions like NO_3^- and NH_4^+ in a ratio of 3:1. However, there was also a significant amount of undetected N, meaning that volatile nitrogenated species such as NO_x or even N_2 are formed, as also mentioned in TiO_2 photocatalysis and EF of anthraquinone dyes [42,45].

3.4. SPEF treatment of simulated DB3 wastewaters

In order to verify the great ability of SPEF catalyzed with 0.5 mM Fe^{2+} + 0.1 mM Cu^{2+} at 50 mA cm^{-2} to decolorize and mineralize DB3 solutions, a synthetic dye wastewater was prepared by mixing 200 mg l^{-1} DB3 with several surfactants and additives, thus simulating effluents from the dyeing process carried out in a Chilean dyehouse. A blank solution prepared without DB3

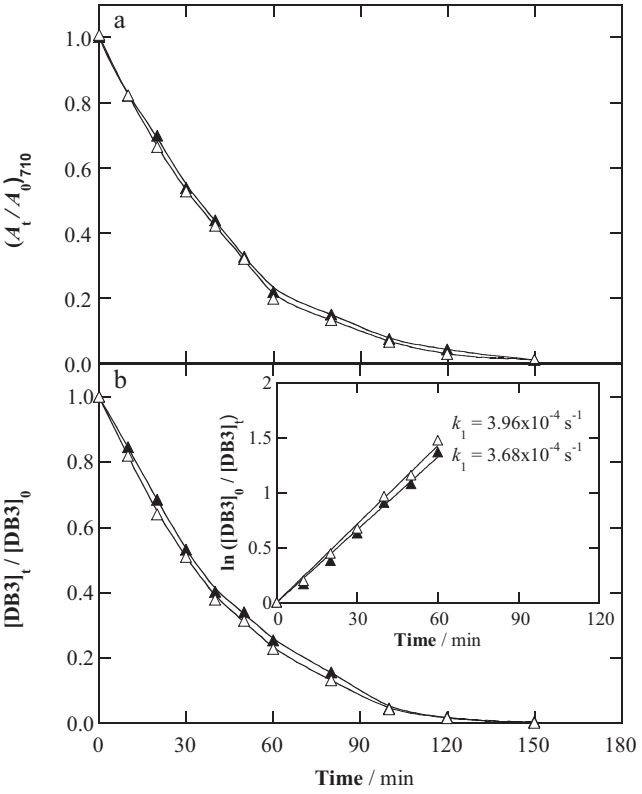

Fig. 7. (a) Normalized absorbance at 710 nm and (b) normalized DB3 concentration vs electrolysis time for the SPEF experiments of Fig. 6 with 200 mg l^{-1} DB3 solution and (▲) 0.5 mM Fe^{2+} or (△) 0.5 mM Fe^{2+} + 0.1 mM Cu^{2+}. In plot (b), the kinetic analysis considering that the dye follows a pseudo first-order reaction and the corresponding rate constants obtained are depicted in the inset panel.

contained 330 mg l^{-1} TOC, which was reduced by 92% at 360 min, as depicted in Fig. 6a. This is certainly important because ensures the quick mineralization of this kind of synthetic organic matter, which usually affects the biodegradability of the effluents and then limits the coupling of the AOPs with bioremediation technologies. In the presence of DB3, the solution contained 430 mg l^{-1} TOC and Fig. 6a shows that it was almost totally mineralized (>95% TOC removal) at 360 min, with only 21 mg l^{-1} TOC still remaining in solution. These results corroborate the ability of the SPEF process to treat highly concentrated effluents, since the almost total TOC removal for a much lower amount of 100 mg l^{-1} TOC required 240 min of electrolysis (see Fig. 2a). The synergistic effect of Cu^{2+} was confirmed again by treating the simulated wastewater by SPEF with Fe^{2+} under similar conditions, which led to a slower mineralization with 89% TOC removal at 360 min (see Fig. 6a).

The EC_{TOC} calculated for the three treatments of Fig. 6a are gathered in Fig. 6b. The treatment of the solutions without DB3 involved a consumption of 87 kWh $(kg\,TOC)^{-1}$ at 360 min, whereas only 69 and 64.5 kWh $(kg\,TOC)^{-1}$ were required for SPEF with Fe^{2+} and Fe^{2+}/Cu^{2+}, respectively. The EC_{TOC} is then much lower than that found for synthetic DB3 solutions in Fig. 2b, indicating that SPEF is very suitable for treating effluents with a high organic load.

The color and DB3 removal were also assessed for the above simulated textile dyeing wastewaters. A practically identical decrease of the normalized absorbance at 710 nm can be seen for both SPEF treatments in Fig. 7a, as was commented from Fig. 3a. It can also be noted that the decolorization kinetics is much slower than that obtained for synthetic DB3 solutions in Fig. 3a. For example, 90% and 99% color removal were achieved for the simulated wastewater after 90 and 150 min, respectively, instead of 30 and 50 min for the analogous DB3 solution. This is due to the so-called matrix effect, i.e., the presence of a larger number of organic molecules that are competing to react with the same concentration of •OH. The EC calculated from Eq. (5) for 90% decolorization is 6.6 kWh m^{-3} (0.40–1.12 €), which is still a competitive value. As expected, the DB3 decay presented in Fig. 7b is quite similar to the absorbance decay because Cu^{2+} does not have a great influence in the oxidation of the aromatic compounds in SPEF. The inset shows that the destruction of DB3 by •OH in a complex matrix agrees with a pseudo first-order kinetics as in the case of synthetic solutions, but exhibits lower pseudo first-order rate constants.

4. Conclusions

The SPEF process with Fe^{2+} is an emerging EAOP that possesses all the characteristics to become a competitive wastewater remediation technology, since it takes advantage of a limitless, natural UV radiation source to oxidize a wide range of dissolved contaminants. Here, the very positive effect of sunlight and Fe^{2+} has been demonstrated for the treatment of an industrial pollutant belonging to a poorly explored family such as the anthraquinonic dyes. The complete decolorization and mineralization of solutions were achieved within relatively short time periods. The co-catalytic role of Cu^{2+} has also been surveyed, which can become an interesting alternative to take advantage of the presence of copper in waters in some environments or in countries with large Cu production like Chile. The best catalytic conditions to accelerate the mineralization process by SPEF were achieved with 0.5 mM Fe^{2+} + 0.1 mM Cu^{2+}, which allowed the easy oxidation of Cu(II)-carboxylate complexes by generated •OH as well as the simultaneous photolysis of the Fe(III) complexes under solar irradiation. A reaction scheme was proposed for DB3 degradation including the fifteen aromatic byproducts identified by GC–MS. The efficacy of SPEF with Fe^{2+}/Cu^{2+} was also ascertained by successfully treating a simulated textile dyeing wastewater.

Acknowledgments

Financial support from FONDECYT – 11090275, DICYT-USACh under project Bicentenario PDA-03, as well as from MICINN (Ministerio de Ciencia e Innovación, Spain) under project CTQ2010-16164/BQU, cofinanced by Feder funds is acknowledged. We are also grateful to the program 'Becas Iberoamérica. Jóvenes Profesores e Investigadores. Santander Universidades'.

References

[1] European Parliament and Council of the European Union, Directive 2000/60/EC of the EP and of the Council of 23 October 2000 establishing a framework for Community action in the field of water policy (00/60/EC), Official Journal of the European Communities, L327/1, 2000.
[2] L. Szpyrkowicz, C. Juzzolino, S.N. Kaul, S. Daniele, M.D. De Faveri, Ind. Eng. Chem. Res. 39 (2000) 3241–3248.
[3] R.M. Christie (Ed.), Environmental Aspects of Textile Dyeing, Woodhead Publ. Ltd., Cambridge, England, 2007.
[4] C.A. Martínez-Huitle, E. Brillas, Appl. Catal. B: Environ. 87 (2009) 105–145.
[5] H.-S. Bien, J. Stawitz, K. Wunderlich, Anthraquinone dyes and intermediates, in: Ullman's Encyclopedia of Industrial Chemistry, vol. 3, Wiley-VCH, Weinheim, Germany, 2003, pp. 207–267.
[6] E. Forgacs, T. Cserháti, G. Oros, Environ. Int. 30 (2004) 953–971.
[7] M. Klavarioti, D. Mantzavinos, D. Kassinos, Environ. Int. 35 (2009) 402–417.
[8] I. Sirés, E. Brillas, Environ. Int. doi:10.1016/j.envint.2011.07.012.
[9] A. Anglada, A. Urtiaga, I. Ortiz, J. Chem. Technol. Biotechnol. 84 (2009) 1747–1755.
[10] M. Panizza, G. Cerisola, Chem. Rev. 109 (2009) 6541–6569.
[11] M. Faouzi, P. Cañizares, A. Gadri, J. Lobato, B. Nasr, R. Paz, M.A. Rodrigo, C. Saez, Electrochim. Acta 52 (2006) 325–331.
[12] L.S. Andrade, L.A.M. Ruotolo, R.C. Rocha-Filho, N. Bocchi, S.R. Biaggio, J. Iniesta, V. García-Garcia, V. Montiel, Chemosphere 66 (2007) 2035–2043.
[13] E. Butrón, M.E. Juárez, M. Solis, M. Teutli, I. González, J.L. Nava, Electrochim. Acta 52 (2007) 6888–6894.
[14] M. Panizza, G. Cerisola, Appl. Catal. B: Environ. 75 (2007) 95–101.

[15] C. Saez, M. Panizza, M.A. Rodrigo, G. Cerisola, J. Chem. Technol. Biotechnol. 82 (2007) 575–581.
[16] J. Sun, H. Lu, L. Du, H. Lin, H. Li, Appl. Surf. Sci. 257 (2011) 6667–6671.
[17] B. Marselli, J. Garcia-Gomez, P.A. Michaud, M.A. Rodrigo, Ch. Comninellis, J. Electrochem. Soc. 150 (2003) D79–D83.
[18] E. Brillas, I. Sirés, M.A. Oturan, Chem. Rev. 109 (2009) 6570–6631.
[19] E. Rosales, M. Pazos, M.A. Longo, M.A. Sanromán, Chem. Eng. J. 155 (2009) 62–67.
[20] I. Sirés, J.A. Garrido, R.M. Rodríguez, P.L. Cabot, F. Centellas, C. Arias, E. Brillas, J. Electrochem. Soc. 153 (2006) D1–D9.
[21] M. Panizza, G. Cerisola, Water Res. 43 (2009) 339–344.
[22] S. Randazzo, O. Scialdone, E. Brillas, I. Sirés, J. Hazard. Mater. 192 (2011) 1555–1564.
[23] S. Hammami, N. Oturan, N. Bellakhal, M. Dachraoui, M.A. Oturan, J. Electroanal. Chem. 610 (2007) 75–84.
[24] A. Lahkimi, M.A. Oturan, N. Oturan, M. Chaouch, Environ. Chem. Lett. 5 (2007) 35–39.
[25] A.R. Khataee, V. Vatanpour, A.R. Amani Ghadim, J. Hazard. Mater. 161 (2009) 1225–1233.
[26] A. Özcan, M.A. Oturan, N. Oturan, Y. Şahin, J. Hazard. Mater. 163 (2009) 1213–1220.
[27] A. Dirany, I. Sirés, N. Oturan, M.A. Oturan, Chemosphere 81 (2010) 594–602.
[28] I. Sirés, C.T.J. Low, C. Ponce-de-León, F.C. Walsh, Electrochem. Commun. 12 (2010) 70–74.
[29] J.M. Peralta-Hernández, Y. Meas-Vong, F.J. Rodríguez, T.W. Chapman, M.I. Maldonado, L.A. Godínez, Water Res. 40 (2006) 1754–1762.
[30] A. Wang, J. Qu, H. Liu, J. Ru, Appl. Catal. B: Environ. 84 (2008) 393–399.
[31] X. Zhang, L. Lei, B. Xia, Y. Zhang, J. Fu, Electrochim. Acta 54 (2009) 2810–2817.
[32] A.R. Khataee, M. Zarei, S. Khameneh Asl, J. Electroanal. Chem. 648 (2010) 143–150.
[33] C. Flox, P.L. Cabot, F. Centellas, J.A. Garrido, R.M. Rodríguez, C. Arias, E. Brillas, Appl. Catal. B: Environ. 75 (2007) 17–28.
[34] M. Skoumal, R.M. Rodríguez, P.L. Cabot, F. Centellas, J.A. Garrido, C. Arias, E. Brillas, Electrochim. Acta 54 (2009) 2077–2085.
[35] E. Guinea, J.A. Garrido, R.M. Rodríguez, P.L. Cabot, C. Arias, F. Centellas, E. Brillas, Electrochim. Acta 55 (2010) 2101–2115.
[36] L.C. Almeida, S. Garcia-Segura, N. Bocchi, E. Brillas, Appl. Catal. B: Environ. 103 (2011) 21–30.
[37] E.J. Ruiz, C. Arias, E. Brillas, A. Hernández-Ramírez, J.M. Peralta-Hernández, Chemosphere 82 (2011) 495–501.
[38] R. Salazar, S. Garcia-Segura, M.S. Ureta-Zañartu, E. Brillas, Electrochim. Acta 56 (2011) 6371–6379.
[39] D. Rajkumar, J. Guk Kim, J. Hazard. Mater. B136 (2006) 203–212.
[40] D. Rajkumar, B. Joo Song, J. Guk Kim, Dyes Pigments 72 (2007) 1–7.
[41] M. Siddique, R. Farooq, Z. Mehmood Khan, Z. Khan, S.F. Shaukat, Ultrason. Sonochem. 18 (2011) 190–196.
[42] B. Gözmen, B. Kayan, A.M. Gizir, A. Hesenov, J. Hazard. Mater. 168 (2009) 129–136.
[43] H. Xu, D. Zhang, W. Xu, J. Hazard. Mater. 158 (2008) 445–453.
[44] J.-M. Fanchiang, D.-H. Tseng, Chemosphere 77 (2009) 214–221.
[45] A. Bianco Prevot, C. Baiocchi, M.C. Brussino, E. Pramauro, P. Savarino, V. Augugliaro, G. Marcì, L. Palmisano, Environ. Sci. Technol. 35 (2001) 971–976.
[46] M. Saquib, M. Muneer, Dyes Pigments 53 (2002) 237–249.
[47] A.R. Kathaee, M. Zarei, M. Fathinia, M. Khobnasab Jafari, Desalination 268 (2011) 126–133.
[48] E. Brillas, M.A. Baños, S. Camps, C. Arias, P.L. Cabot, J.A. Garrido, R.M. Rodríguez, New J. Chem. 28 (2004) 314–322.
[49] C. Flox, S. Ammar, C. Arias, E. Brillas, A.V. Vargas-Zavala, R. Abdelhedi, Appl. Catal. B: Environ. 67 (2006) 93–104.
[50] H. Gallard, J. De Laat, B. Legube, Rev. Sci. Eau 12 (1999) 713–728.
[51] Comisión Nacional de la Energía (http://www.cne.es/cne/Home), based on Boletín Oficial del Estado N° 156 (BOE-A-2011-11267, 1 July 2011).
[52] C. Lizama, J. Freer, J. Baeza, H.D. Mansilla, Catal. Today 76 (2002) 235–246.